# Indiscriminate Binding by Orotidine 5′-Phosphate Decarboxylase of Uridine 5′-Phosphate Derivatives with Bulky Anionic $C_6$ Substituents†

Charles A. Lewis, Jr. and Richard Wolfenden*

*Department of Biochemistry and Biophysics, University of North Carolina at Chapel Hill, Chapel Hill, North Carolina 27599*

*Received April 26, 2007; Revised Manuscript Received September 11, 2007*

ABSTRACT: Orotidine 5′-phosphate (OMP) decarboxylase appears to act upon its substrate without the intervention of metals or other cofactors and without the formation of covalent bonds between the enzyme and the substrate. Crystallographic information indicates that substrate binding forces the substrate's scissile carboxylate group into the neighborhood of several charged groups at the active site. It has been proposed that binding might result in electrostatic stress at the substrate's $C_6$ carboxylate group in such a way as to promote decarboxylation by destabilizing the enzyme−substrate complex in its ground state. If that were the case, one would expect uridine 5′-phosphate (UMP) derivatives with bulky anionic substituents at $C_6$ to be bound weakly compared with UMP, which is unsubstituted at $C_6$. Here, we describe the formation of anionic 5,6-dihydro-6-sulfonyl derivatives by spontaneous addition of sulfite to UMP and to OMP. These sulfite addition reactions, which are slowly reversible and are not catalyzed by the enzyme, result in the appearance of one (or, in the case of OMP, two) bulky anionic substituents at the 6-carbon atom of UMP. These inhibitors are bound with affinities that surpass the binding affinity of UMP. We are led to infer that the active site of OMP decarboxylase is remarkably accommodating in the neighborhood of $C_6$. These are not the properties that one would expect of an active site with a rigid structure that imposes sufficient electrostatic stress on the substrate to produce a major advancement along the reaction coordinate.

In the final step of pyrimidine nucleotide biosynthesis (Scheme 1), the dimeric enzyme orotidine 5′-phosphate decarboxylase (ODCase;[1] E.C. 4.1.1.23) converts orotidine 5′-phosphate (OMP) to uridine 5′-phosphate (UMP) with the release of $CO_2$. Unlike most decarboxylases, ODCase contains no metal ions or other cofactors that might contribute to catalysis, and there is no evidence that this reaction proceeds through a covalent intermediate (*1*). One mechanism that has been proposed (*2*) for this reaction involves electrostatic stress between the scissile 6-carboxylate group of OMP and the carboxylate groups of two active site residues (Asp-91 and Asp-96 of the yeast sequence). These residues recur, with Lys-59 and Lys-95, as members of a conserved quartet of charged residues that are present in ODCase in organisms from every kingdom (*3*). In the crystal structures of nucleotide complexes with ODCase, the 5′-phosphoryl group appears to brace the substrate within the active site in such a way as to force the scissile carboxylate group into the neighborhood of the charged quartet. Removal of the 5′-phosphoryl group from OMP reduces its susceptibility to enzymatic decarboxylation by a startling factor of $10^{11}$, indicating a contribution to the rate enhancement whose magnitude exceeds the effects of a single substituent that appear to have been recorded for any other enzyme reaction (*4*, *5*).

Scheme 1: Decarboxylation of OMP to UMP Catalyzed by ODCase

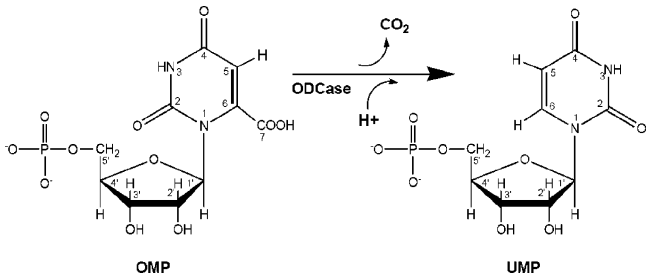


It is not a simple matter to test the electrostatic stress hypothesis directly. Enzyme complexes with the product UMP have been characterized extensively, but enzyme-bound OMP is kinetically and thermodynamically unstable and has been observed only after mutation of active site residues that are essential for catalysis (*6*, *7*). An alternative approach, adopted in the present work, is to examine the enzyme's affinity for substrate analogues whose structures would be expected to accentuate or alleviate stress. Earlier, 6-methylamino-UMP, with a potential positive charge at the position normally occupied by the scissile carboxylate group of OMP, was shown to be bound in uncharged form with an affinity that approaches the affinity of OMP itself (*8*).

† This work was supported by National Institutes of Health Grant GM-18325.

* To whom correspondence should be addressed. Phone: (919) 966-1203. Fax: (919) 966-2852. E-mail: water@med.unc.edu.

[1] Abbreviations: ODCase, orotidine 5′-monophosphate decarboxylase; OMP, orotidine 5′-monophosphate, UMP, uridine 5′-monophosphate; MOPS, 3-morpholinopropanesulfonic acid; UMP-$SO_3$, 5,6-dihydro-UMP-6-sulfonate; OMP-$SO_3$, 5,6-dihydro-OMP-6-sulfonate; H-UMP-$SO_3$, (5-H,5-H)-5,6-dihydro-UMP-6-$SO_3$; D-UMP-$SO_3$, (5-D,5-H)-5,6-dihydro-UMP-6-$SO_3$; H-OMP-$SO_3$, (5-H,5-H)-5,6-dihydro-OMP-6-$SO_3$; D-OMP-$SO_3$, (5-D,5-H)-5,6-dihydro-OMP-6-$SO_3$.

10.1021/bi700796t CCC: $37.00 
Published on Web 10/30/2007

Scheme 2: Sulfite Addition to (A) UMP and (B) OMP

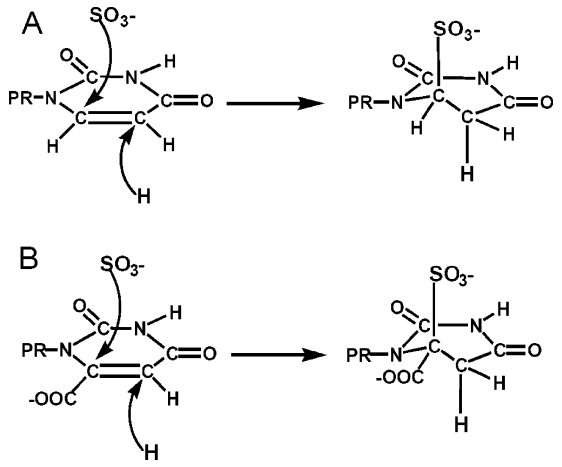

If electrostatic stress were to destabilize the enzyme−OMP complex in such a way as to reduce the thermodynamic barrier that must be surmounted to reach the transition state, then nonreacting analogues bearing negatively charged substituents at $C_6$ would be expected to be less tightly bound by the enzyme than analogues lacking those substituents. Pyrimidine derivatives have been shown to undergo 6-addition of the sulfite anion, an exceptionally reactive nucleophile, with *trans* addition of a solvent proton at $C_5$ (*9*−*16*) (Scheme 2A). Sulfite addition to UMP seemed to offer an opportunity to prepare an analogue of OMP equipped with a bulkier anionic substituent than the 6-carboxylate group of OMP. Examining the scope of this reaction, we were surprised to find that OMP also undergoes sulfite addition at $C_6$, albeit less readily than UMP, yielding a molecule with *two* anionic substituents at the 6-position (Scheme 2B). Here, we describe the preparation of these analogues and their behavior as inhibitors of ODCase.

## MATERIALS AND METHODS

*Materials.* Nucleotides and other reagents were purchased from Sigma-Aldrich Chemical Corp. Yeast ODCase C155S, a mutant enzyme that is more stable than the wild-type enzyme but retains its catalytic properties, was kindly provided by Dr. Steven Short of GlaxoSmithKline, Research Triangle Park, NC 27709.

*Preparation of Adducts.* Sulfite mixtures containing equimolar $NaHSO_3$ and $Na_2SO_3$ (pH 7.0) were used in addition reactions. Addition of sulfite to UMP was conducted in $H_2O$ or $D_2O$ to produce adducts with two protons at $C_5$ or one proton and one deuteron at $C_5$, respectively. Adducts of UMP were prepared by exposing UMP (0.025 M) to sulfite (0.6 M) for 24 h at room temperature, allowing addition to proceed to completion as described for the corresponding uracil derivatives (*9*, *13*). Sulfite addition to OMP required higher sulfite concentrations and higher temperatures than sulfite addition to UMP. OMP adducts were prepared by exposing OMP (∼0.010 M) to sulfite (2.0 M) at 40 °C for 3 days. Unexpectedly, this reaction was found to proceed to completion after the resulting solution had been stored frozen for several days (see the Results).

*$^1$H NMR Spectroscopy.* $^1$H NMR spectra were obtained using Varian Unity Inova 500 and 600 MHz spectrometers (Palo Alto, CA) controlled by Solaris 9 software. Samples were generally analyzed at a concentration of $\sim 3 \times 10^{-3}$ M in $D_2O$ at 25 °C, acquiring 16 transients, and spectra were referenced to the chemical shift of the residual water proton resonance at 4.77 ppm.

The time course of formation of the two diastereomeric adducts of UMP and OMP was followed by $^1$H NMR. Integrated intensities of the resonances arising from the $C_6$, $C_5$, and $C_{1'}$ protons of UMP and the $C_5$, and $C_{1'}$ protons of OMP, for each diastereomer and unreacted nucleotide, were substituted into eq 1 (*17*) to calculate the concentrations of

$$[\mathrm{I}] = ([\mathrm{Int_I}]/[\mathrm{Int_I} + \mathrm{Int_{II}} + \mathrm{Int_{nuc}}])[\mathrm{nucleotide_t}] \quad (1)$$

each diastereomer and unreacted nucleotide at each time point. $Int_I$ is the integrated intensity of the signal arising from diastereomer I, $Int_{II}$ and $Int_{nuc}$ are those of diasteromer II and unreacted nucleotide, and $[nucleotide_t]$ is the concentration of nucleotide at the start of the experiment.

At each time point, the concentration of sulfite remaining was calculated by subtracting the sum of the concentrations of the two diastereomers of the adduct from the initial sulfite concentration. Changes in the concentration of sulfite, which was present in large excess, were negligible. At this stage, no correction was made for the state of ionization of sulfite at pH 7. From the above concentrations, apparent equilibrium constants for the formation of each adduct, at each time point, were calculated using eq 2 (*17*), where $K_{app}$ is the apparent

$$K_{\mathrm{app}} = [\mathrm{X}]_t/[\mathrm{nucleotide}]_t[\mathrm{sulfite}]_t \quad (2)$$

equilibrium constant for formation of the adduct at time *t* and $[X]_t$, $[nucleotide]_t$, and $[sulfite]_t$ are the concentrations of adduct, unreacted nucleotide, and sulfite at that time point.

*Kinetics of Sulfite Addition.* To reduce interference between the UV absorbance of sulfite and the UV absorbance of the nucleotides in experiments to determine the rate of sulfite addition to UMP and OMP spectrophotometrically, it was necessary to reduce the sulfite concentration to values lower than those used in the preparative work. Reaction mixtures containing UMP or OMP ($10^{-4}$ M) and sulfite (pH 7.0, 0.06−0.50 M) were monitored at 276 nm, using a Hewlett-Packard 8452A diode array spectrophotometer.

*ODCase Inhibition.* The action of ODCase was monitored spectrophotometrically at 279 nm by published procedures (*5*, *18*) with minor modification. The reaction was initiated by adding ODCase (10 $\mu$L, $\sim 3 \times 10^{-9}$ M in monomer, in 0.1 M NaCl) to a mixture (1 mL) containing OMP ($(1-8) \times 10^{-5}$ M) and MOPS buffer (0.01 M, pH 7.2). Hewlett-Packard UV−vis ChemStation software was used to obtain a zeroth-order fit to absorbance data. Plots of [substrate]/velocity vs [substrate] were constructed using Excel. Solving the equations for $y = 0$ yielded the $x$ intercept, representing $-K_m$ (or $-K_p$ when the inhibitor was present), and the slope yielded $1/V$. In each case, inhibition was found to be competitive (see the Results), and inhibition constants were calculated using eq 3, where $i$ is the concentration of the

$$K_{\mathrm{i}} = i/[(K_{\mathrm{p}}/K_{\mathrm{m}}) - 1] \quad (3)$$

adduct being tested, $K_p$ is the apparent $K_m$ value of OMP in the presence of inhibitor, and $K_m$ is the $K_m$ value of OMP in the absence of inhibitor.

Table 1: $^1$H NMR Resonances for Sulfite Addition to UMP[a,b]

| | (5-H,5-H)-5,6-Dihydro-UMP-6-$SO_3$ (H-UMP-$SO_3$) | | | | | | | |
|---|---|---|---|---|---|---|---|---|
| | diastereomer I (49.4%) | | | | diastereomer II (50.6%) | | | |
| | $C_{1'}H$ | $C_6H_X$ | $C_5H_A$ | $C_5H_B$ | $C_{1'}H$ | $C_6H_X$ | $C_5H_A$ | $C_5H_B$ |
| chemical shift | 5.81 (d) | 5.04 (d) | 3.30 (dd) | 3.07 (d) | 5.25 (d) | 4.91 (d) | 3.18 (dd) | 3.03 (d) |
| coupling, Hz | 5.5 | 7.1 | 7.1, 17.7 | 17.7 | 1.8 | 6.7 | 6.8, 17.7 | 17.7 |
| separation of $C_5H$'s, Hz | | | 115 | | | | 75 | |
| | (5-D,5-H)-5,6-Dihydro-UMP-6-$SO_3$ (D-UMP -$SO_3$) | | | | | | | |
| | diastereomer I (52.2%) | | | | diastereomer II (47.8%) | | | |
| | $C_{1'}H$ | $C_6H_X$ | $C_5H_A$ | $C_5H_B$ | $C_{1'}H$ | $C_6H_X$ | $C_5H_A$ | $C_5H_B$ |
| chemical shift | 5.81 (s) | 5.04 (s) | | 3.07 (s) | 5.26 (s) | 4.91 (s) | | 3.05 (s) |
| coupling, Hz | 5.0 | N/A | | N/A | N/A | N/A | | N/A |

[a] The chemical shifts, multiplicity, and coupling constants for comparable UMP protons are ($C_{1'}H$) 5.96 (d), 6.05 Hz, ($C_5H$) 5.95 (d), 8.5 Hz, and ($C_6H$) 8.1 (d), 8.5 Hz. s = singlet, d = doublet, and dd = doublet of doublets. [b] The composition of the adduct mixture is given as a percentage for each diastereomer.

Table 2: $^1$H NMR Resonances for Sulfite Addition to OMP[a,b]

| | (5-H,5-H)-5,6-Dihydro-OMP-6-$SO_3$ (H-OMP-$SO_3$) | | | | | |
|---|---|---|---|---|---|---|
| | diastereomer I (35.6%) | | | diastereomer II (64.4%) | | |
| | $C_{1'}H$ | $C_5H_A$ | $C_5H_B$ | $C_{1'}H$ | $C_5H_A$ | $C_5H_B$ |
| chemical Shift | 5.18 (d) | 3.32 (d) | 3.27 (d) | 5.08 (s) | 3.40 (d) | 3.26 (d) |
| coupling, Hz | 2.3 | 17.4 | 17.4 | N/A | 17.6 | 17.6 |
| separation of $C_5H$'s, Hz | | 24.8 | | | 66.2 | |
| | (5-D,5-H)-5,6-Dihydro-O MP-6-$SO_3$ (D-OMP-$SO_3$)[c] | | | | | |
| | diastereomer I (29.4%) | | | diastereomer II (70.6%) | | |
| | $C_{1'}H$ | $C_5H_A$ | $C_5H_B$ | $C_{1'}H$ | $C_5H_A$ | $C_5H_B$ |
| chemical shift | 5.14 (d) | | 3.24 (s) | 5.02 (s) | | 3.2 (s) |
| coupling, Hz | 2.3 | | N/A | N/A | | N/A |

[a] The chemical shifts, multiplicity, and coupling constants for comparable OMP protons are ($C_{1'}H$) 5.45 (d), 2.4 Hz, and ($C_5H$) 5.71 (s). s = singlet, and d = doublet. [b] The composition of the adduct mixture is given as a percentage for each diastereomer. [c] The deuterated OMP-$SO_3$ contained a small amount of protio-OMP-$SO_3$, rendering it difficult to obtain good integrated areas for $C_5$ protons. However, the relative integrated intensities of the $C_{1'}$ and $C_5$ protons were comparable in magnitude.

## RESULTS

*$^1$H NMR of UMP and OMP Adducts.* The proton resonances observed for the sulfite addition products of UMP and OMP are listed in Tables 1 and 2. In the case of UMP-$SO_3$, the signals arising from the vinyl protons at $C_5$ and $C_6$ of the pyrimidine ring are replaced by those of the aliphatic protons of the 5,6-dihydro species. Because chiral centers are present in both substituent ribose and $C_6$ of the saturated pyrimidine ring, diastereomeric products would be expected to result from sulfite addition (*9*, *17*, *19*) and were observed in the present experiments. Here, we refer to these diastereomers as I and II, the resonances of I appearing downfield from those of II. The nonequivalent protons at $C_5$ (A and B) and the single proton at $C_6$ (X) constitute an ABX spin system.

Sulfite addition to UMP was accompanied by a change in the chemical shift of the $C_6$ proton, and two new resonances were observed. The signals attributed to $C_5$ (A and B) each exhibited a doublet structure, with a characteristically large geminal coupling constant (~17 Hz) like those of the $C_5$ protons of 5,6-dihydroorotic acid and its methyl ester (*20*). One of the $C_5$ protons ($C_{5A}$) was also coupled to the $C_6$ proton, generating a doublet of doublets. Parts A and B of Figure 1 show the 600 MHz spectrum of the UMP adducts.

Table 1 shows the $^1$H NMR data for the protons at $C_5$, $C_6$, and $C_{1'}$ of the ribose of the UMP adducts along with the relative concentrations of the two diastereomers of the adduct, based on comparison of the integrated resonances corresponding to the protons at $C_6$, $C_5$, and $C_{1'}$. For simplicity, the 2′, 3′, 4′, and 5′ ribose protons are not included in Table 1.

When the sulfonate adduct of UMP was prepared in $D_2O$, the proton NMR spectrum (Figure 1B) showed that deuteration had occurred at $C_5$. The complex doublet of doublets, corresponding to the $C_{5A}$ proton of each diastereomer, was lost, and two singlets remained at 3.07 and 3.05 ppm, corresponding to the $C_{5B}$ protons. In addition, the resonances of the $C_{6X}$ protons collapsed to singlets, because the coupling to the deuteron at $C_5$ is very small. That observation confirmed the assignment of the complex doublet of doublets at 3.35 and 3.25 ppm to the proton added during sulfite addition. The anomeric $C_{1'}$ proton was unaffected by deuteration at $C_5$. The change in the relative populations of the two diastereomers, between the protio and deuterio adducts, was very slight, amounting to ~3%.

The spectra of the sulfonate adducts of OMP show the absence of a resonance for a $C_6$ proton, or coupling to a $C_5$ proton, confirming that sulfite addition occurred at $C_6$ (as in the case of UMP) rather than at $C_5$. Proton resonances were observed that correspond to two diastereomers, for the anomeric ribose $C_{1'}$ proton and the $C_5$ protons (Figure 2A). The $C_5$ protons of the adducts also showed the ~17 Hz geminal coupling constant observed for the UMP-$SO_3$ adducts in the present work and as reported earlier for 5,6-dihydroorotic acid (*20*). In the OMP adducts, the signals arising from the $C_5$ protons (A and B) of the two diastereomers overlapped extensively, with less separation between the doublets of the two $C_5$ protons than in the case of the UMP adducts, so that the diastereomer I doublets lie within the larger doublets of diastereomer II. The preparation of OMP-$SO_3$ in $D_2O$ resulted in the expected loss of the $C_{5A}$ protons of the two diastereomers, and the $C_{5B}$ proton doublets each collapsed to a single resonance, shifted from their original positions in the protio-OMP-$SO_3$ adducts as shown

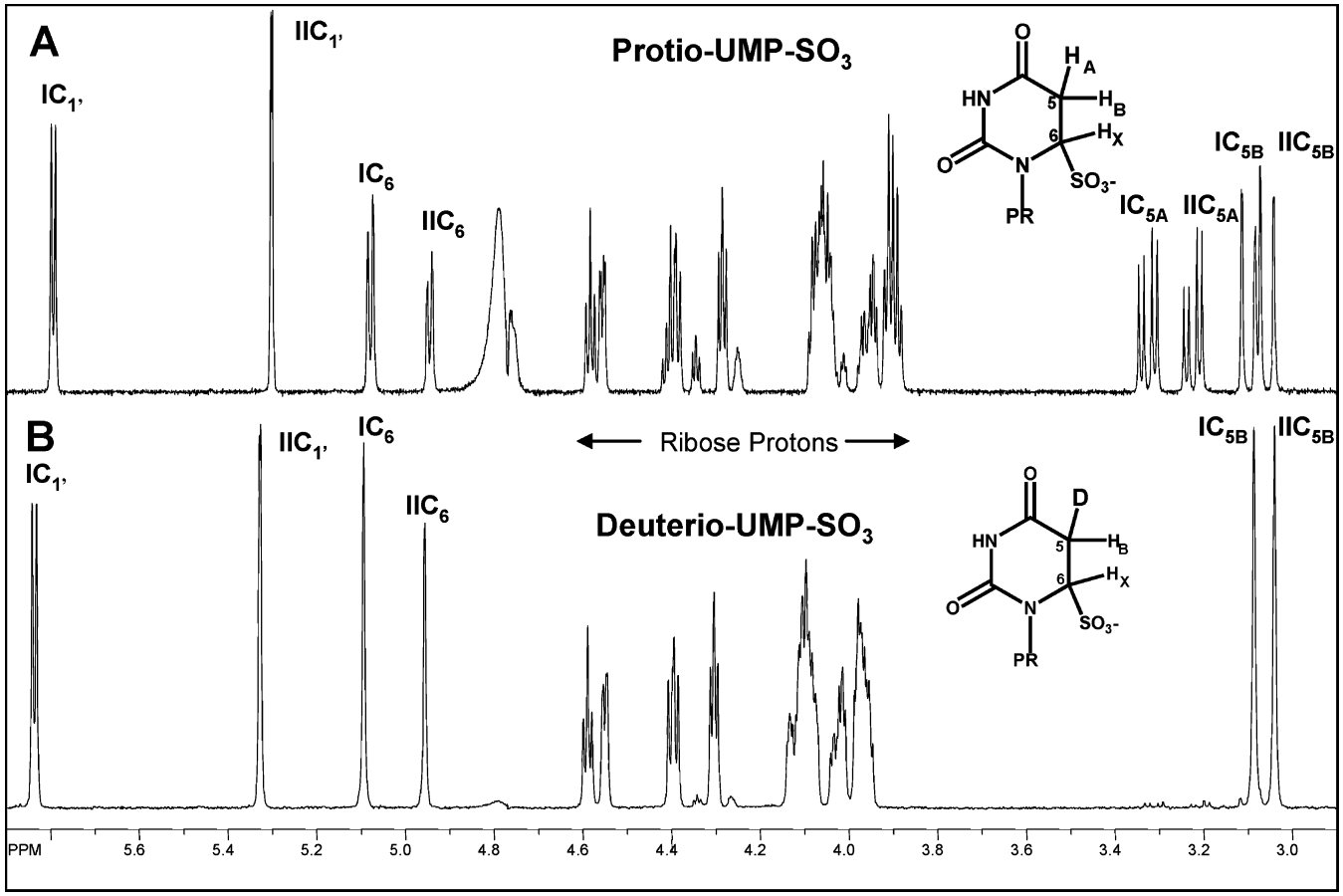


FIGURE 1: $^1$H NMR (600 MHz) spectrum of sulfonate adducts of UMP: (A) Protio-UMP-$SO_3$ prepared in $H_2O$, spectrum recorded in $D_2O$; (B) deuterio-UMP-$SO_3$ prepared in $D_2O$, spectrum recorded in $D_2O$. The two diastereomers of each adduct are indicated by I and II. Resonances of the $C_{1'}$, $C_5$, and $C_6$ protons are identified for each diastereomer. Note the doublet of doublets in the protio adduct for the $C_{5A}$ proton which was added concurrently at $C_5$ with the addition of $SO_3$ at $C_6$. The $C_{5A}$ proton is coupled to the $C_{5B}$ (large splitting) and $C_6$ (small splitting) protons. In the deuterio adduct, the $C_{5A}$ proton was replaced by deuterium in the course of the addition reaction.

in Figure 2 and Table 2. Unlike UMP-$SO_3$ in which the two diastereomers were present in essentially equal amounts, the OMP-$SO_3$ adducts exhibited a distinct preference for diastereomer II over diastereomer I. Thus, the introduction of a *second* bulky group at $C_6$ (the carboxyl and sulfonyl groups) results in a preference for one diastereomer over the other.

The absolute axial/equatorial conformations of substituents in these sulfonate adducts remain to be determined. In dihydro derivatives of uracil and orotic acid derivatives, Katritzky et al. (*20*) found that $C_6$ carboxyl groups preferred the axial position even as their methyl esters, whereas $C_6$ methyl groups in dihydrouracils preferred the equatorial position. Those authors concluded that the shapes and sizes of substituent groups are important in determining conformational equilibria (*20*). The X-ray crystal structure of sodium 5,6-dihydrouracil-6-sulfonate, reported by Barnes and Hawkinson (*21*), shows the $C_6$ sulfonate group is attached axially to the saturated pyrimidine ring. It seems reasonable to conjecture that, in the present UMP-$SO_3$ adducts, the sulfonyl group tends to adopt an axial position.

Figure 3 shows that sulfite addition to UMP proceeds much more rapidly than sulfite addition to OMP. Sulfite addition to UMP proceeded nearly to completion at room temperature (Figure 3A), yielding the two diastereomers in constant proportions that remained unchanged after prolonged freezing. In the case of OMP, the ratio of diastereomers remained constant during the course of the reaction at 40 °C, but the proportion of diastereomer II increased considerably after frozen storage (Figure 3B).[2,3]

Equilibria of sulfite addition were very different for UMP and OMP. Apparent equilibrium constants observed for sulfite addition to OMP were 1.9 and 4.9 $M^{-1}$, respectively, for diastereomers I and II (Figure 4). Apparent equilibrium constants for sulfite addition to UMP were 26 and 27 $M^{-1}$ for diastereomers I and II, respectively. Earlier, Triplett et al. (*17*) used $^{13}$C NMR resonance intensities to estimate equilibrium constants of 6.9 and 7.2 $M^{-1}$ for addition of sulfite (1 M) to UMP (1 M) after 24 h at room temperature. The conditions employed by those investigators were dif-

[2] The addition of $NaHSO_3$ to OMP was incomplete but was rendered more favorable by heating the reaction to 40 °C. Serendipitously, frozen storage drove the reaction further to completion, presumably by increasing the relative concentrations of the two reactants in the unfrozen solution as the water froze.

[3] The amount of remaining OMP in Figure 3B was ~1.5 mM. The dilution of the frozen stock solution and its subsequent dilution into the assay mixture was such that the final concentration of OMP was 4.65, 3.16, and 1.56 $\mu$M for the 60, 40, and 20 $\mu$M H-OMP-$SO_3$ levels. These micromolar amounts of OMP would not have been detected in the rate tracings at 279 nm, since OMP would have been rapidly consumed by the ODCase. The summing of the OMP from the OMP-sulfonate adduct and the OMP added as substrate solution produced no significant differences in calculated $K_i$ values (Figure 9).

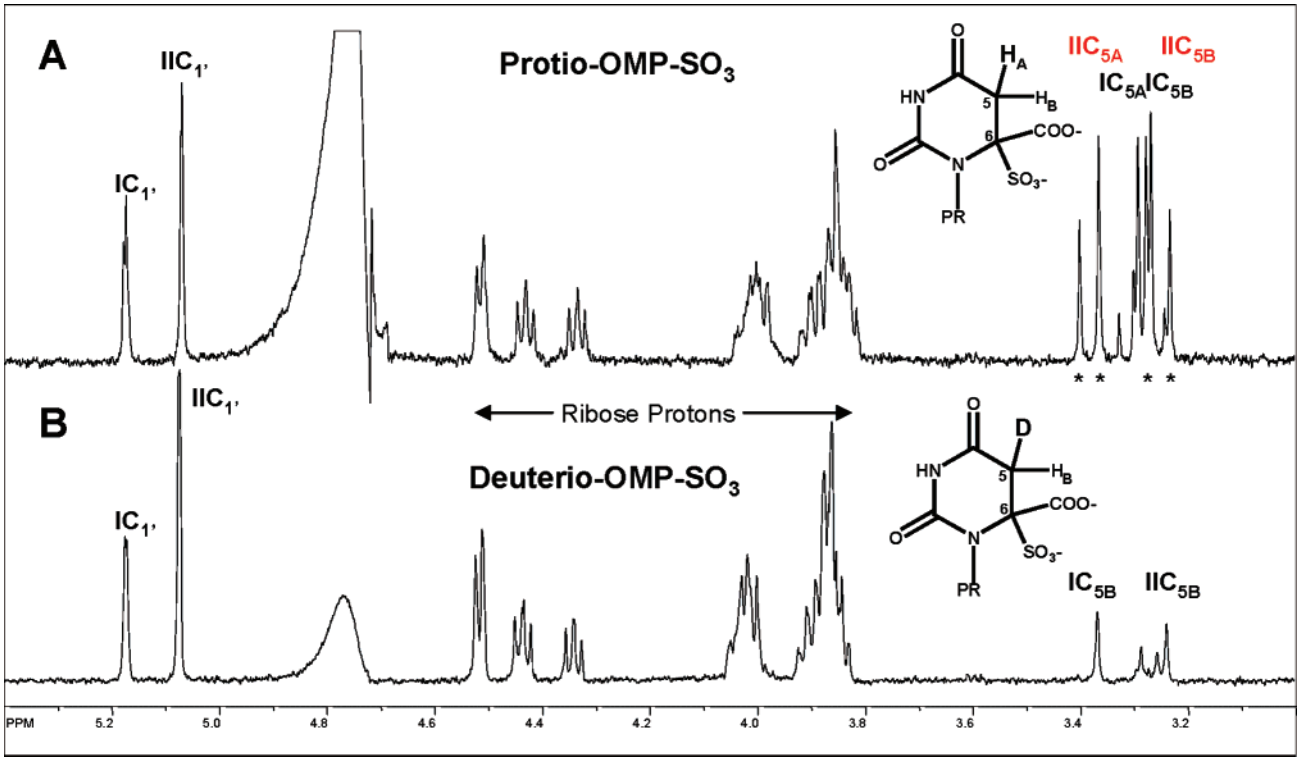


FIGURE 2: $^1$H NMR (500 MHz) spectrum of sulfonate adducts of OMP: (A) Protio-OMP-$SO_3$ prepared in $H_2O$, spectrum recorded in $D_2O$; (B) deuterio-OMP-$SO_3$ prepared in $D_2O$, spectrum recorded in $D_2O$. The two diastereomers of each adduct are indicated by I and II. Resonances of the $C_{1'}$ and $C_5$ protons are identified for each diastereomer. Note the two doublets in the protio adduct for the $C_{5A}$ and $C_{5B}$ protons for diastereomers II (with the large separation and marked with asterisks below the peaks), while the two doublets for the $C_{5A}$ and $C_{5B}$ protons for diastereomer I are closer together and are within the resonances of diastereomer II. In the deuterio adduct, the $C_{5A}$ proton was replaced by deuterium in the course of the addition reaction.

ferent from those in the present experiments, in which the concentration of nucleotide was very much lower.

*Rates of Sulfite Addition.* To minimize the effect of sulfite absorption, UV changes were monitored at 276 nm. Whereas UMP reacted with sulfite nearly to completion in the presence of 0.25 M sulfite after 5 h, the reaction with OMP had progressed only ~4% after 7 h (Figure 5). The difference between the reaction rates of UMP and OMP remained constant over the range of sulfite concentrations tested, UMP reacting approximately 37-fold more rapidly than OMP (Figure 6).

*Inhibition by Unreacted Sulfite*. Inorganic sulfite was evaluated as a potential inhibitor of ODCase over a concentration range of 0.02−0.10 M, well in excess of the level of unreacted sulfite that might remain as a contaminant in the assays from adduct solutions that were tested for nucleotide inhibition (Figure 7). These experiments established an average $K_i$ value of 2.4 mM for sulfite, several orders of magnitude higher than the $K_i$ values of the nucleotide−sulfite adducts. Those findings render it unlikely that residual sulfite could have been responsible for the inhibition observed in the present experiments.

*Inhibition by Sulfonate Adducts of UMP and OMP*. Before the sulfonate adducts of UMP and OMP were tested for inhibitory activity, several potential pitfalls were considered.

(1) The nucleotide−sulfonate adducts might be intrinsically unstable. However, solutions of nucleotide adducts at concentrations of $10^{-3}$ M or greater showed no signs of decomposition after 1 day at room temperature, while enzyme activity measurements were conducted over a period of minutes.

(2) The nucleotide−sulfonate adducts might dissociate spontaneously at the high dilutions that were present in the inhibition experiments. That was shown not to be the case by performing control experiments in which adducts were diluted into an assay buffer at concentrations equivalent to the concentrations of substrate that would be used in assays of activity. When the absorbance at 279 nm was monitored over 10 min, exceeding the time for the enzyme assay, no change was observed. If the adducts had been dissociating with release of sulfite, an increase in absorbance at 279 nm would have been observed, due to formation of the $C_5$═$C_6$ double bond.

(3) ODCase might use the sulfonate adduct of OMP as a substrate, with concomitant release of sulfite. That possibility was tested by incubating the enzyme with a reaction mixture containing buffer and the OMP−sulfonate adduct, but without the addition of substrate OMP. No change in absorbance was observed. If ODCase had acted on the sulfonate adduct of OMP (or catalyzed the release of sulfite from the adduct), followed by reaction of the enzyme with the OMP released, then one would have expected a decrease in absorbance associated with the breakdown of OMP. The total absence of such changes indicated that none of the sulfonate adducts are substrates for ODCase.

After these control experiments had been performed, the diastereomeric mixtures of the sulfonate adducts formed from UMP and OMP were tested as inhibitors of ODCase (Table 3). In both cases, plots of $[S]/v$ vs $[S]$ showed parallel lines in the presence of inhibitors, indicating competitive inhibition (Figures 8 and 9). $K_i$ values for UMP-$SO_3$ adducts were about 7-fold lower than the $K_i$ value for UMP (Table 3). The

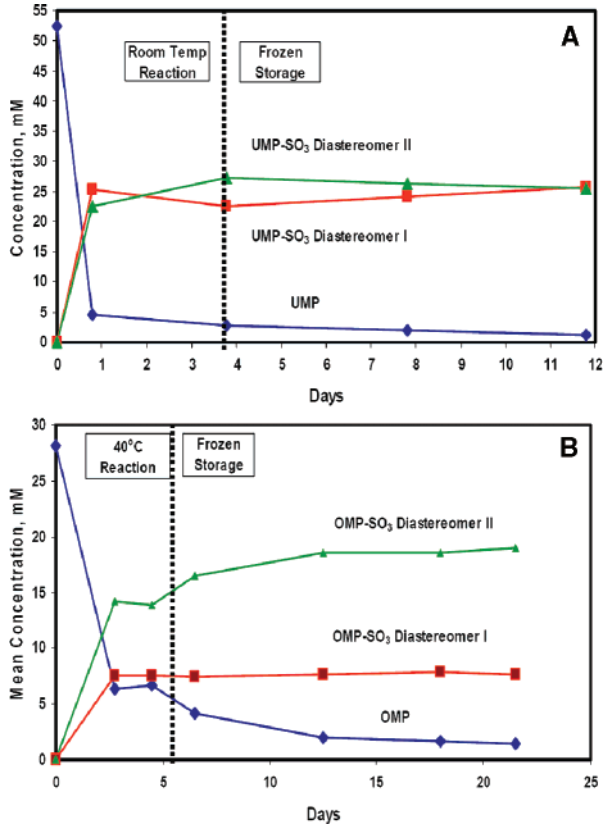


FIGURE 3: (A) Addition of sulfite to UMP monitored by $^1$H NMR. A solution of UMP (0.052 M) was reacted with $NaHSO_3$ (0.6 M) at pH 7. The first 3 days of reaction were conducted at 25 °C, followed by 8 days at −20 °C. Note the constant proportion of the two diastereomers. (B) Addition of sulfite to OMP monitored by $^1$H NMR. A solution of OMP (0.028M) was reacted with $NaHSO_3$ (2.0 M) at pH 7. The first 5 days of reaction were conducted at 40 °C, followed by 17 days at −20 °C. Note the constant amount of diastereomer I and the increasing amount of diastereomer II observed upon frozen storage.

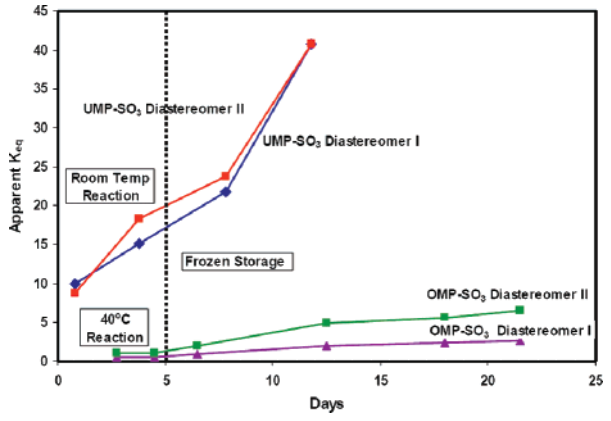


FIGURE 4: Mean apparent $K_{eq}$ values for sulfite addition to UMP and OMP calculated from the $^1$H NMR time course data in Figure 3. UMP-$SO_3$ adduct diastereomers, present in approximately equal amounts as the reaction goes to completion, have nearly equivalent $K_{eq}$ values. OMP-$SO_3$ shows a preference for diastereomer II, which is reflected in different $K_{eq}$ values.

inhibition produced by sulfonate adducts of UMP was free from potential artifacts arising from unreacted UMP, since UMP is bound by the enzyme much less tightly, and any residual UMP would have been present at vanishingly low levels.

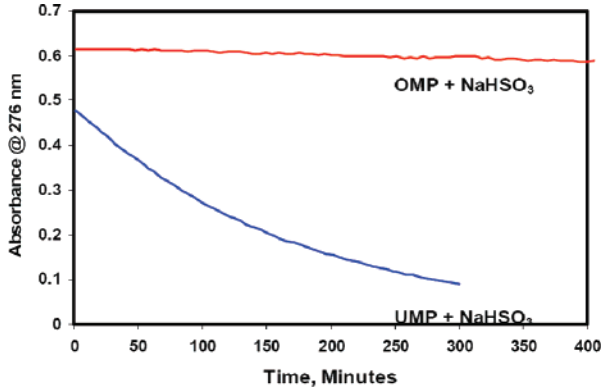


FIGURE 5: UV absorbance changes measured at 276 nm during the reaction of $NaHSO_3$ (0.25 M) at pH 7 with UMP or OMP ($1 \times 10^{-4}$ M) monitored over 5 and 7 h, respectively.

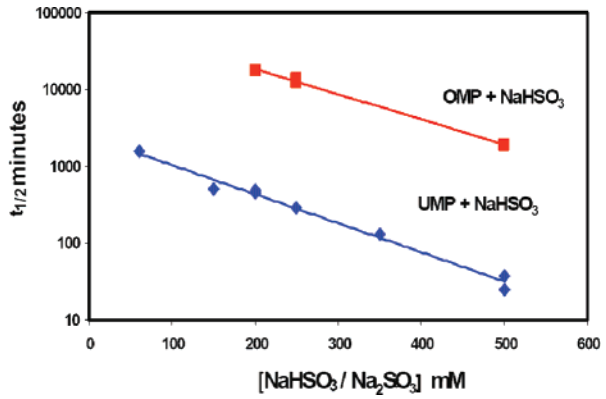


FIGURE 6: Comparison of $t_{1/2}$ for the reaction of UMP or OMP over a range of $NaHSO_3$ concentrations at pH 7. OMP reacted with sulfite about 37-fold slower than UMP.

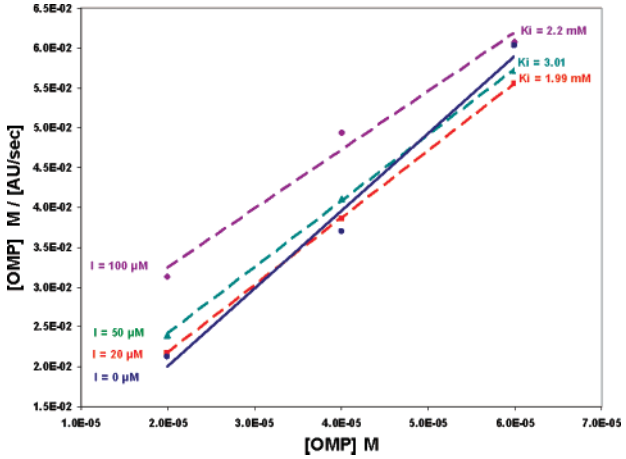


FIGURE 7: Sulfite inhibition of ODCase. Potential inhibition of ODCase by excess sulfite present in the adduct inhibitor solutions was evaluated at final assay concentrations of 20, 50, and 100 mM. These levels are far higher than the ∼3 mM present in the H-UMP-$SO_3$ and ∼2.1 to ∼6.2 mM present in the H-OMP-$SO_3$ inhibition assays. The weak inhibition observed from sulfite has an average $K_i$ value of 2.4 ± 1.6 mM.

The sulfonate adducts of OMP were bound with higher affinity than those of UMP, but less tightly than OMP itself ($K_s = 7 \times 10^{-7}$ M) (*4*, *18*). For the sulfonate adducts of OMP, unreacted OMP might interfere with the assay, at least in principle, since its $K_m$ value is lower than the $K_i$ values of the adducts. However, as noted above, no change in absorbance at 279 nm was observed when OMP adducts were

Table 3: Inhibition of ODCase by Sulfonate Adducts of UMP and OMP

| derived from | sulfite adduct | $K_i$ ($\mu$M) |
|---|---|---|
| UMP ($K_i = 200\ \mu$M) | UMP-$SO_3$ | $29.2 \pm 6.8$ |
| OMP ($K_m = 0.7\ \mu$M) | OMP-$SO_3$ | $20.80 \pm 5.7$ |

exposed to the enzyme in the absence of added OMP substrate. Further, when $K_i$ values were recalculated to allow for residual OMP (~5%) that might be present in the adducts, the change in the calculated $K_i$ value was less than the standard deviation (Figure 9B). Those findings suggest that the inhibition reported for the OMP-$SO_3$ adducts was not due to contaminating OMP.

## DISCUSSION

*Comparison of Binding Affinities*. The sulfonate adducts of both UMP (UMP-$SO_3$) and OMP (OMP-$SO_3$) are effective competitive inhibitors of ODCase, with $K_i$ values that range between $2.0 \times 10^{-5}$ and $2.9 \times 10^{-5}$ M. UMP-$SO_3$ can be considered an analogue of OMP, with a saturated $C_5-C_6$ bond and a sulfonyl group replacing the 6-carboxyl group. UMP-$SO_3$ is bound by yeast ODCase with an affinity ($K_i = 2.9 \times 10^{-5}$ M) that is higher than that of the reaction product UMP ($K_i = 2 \times 10^{-4}$ M) but lower than that of 5,6-dihydro-OMP ($K_i = 2.5 \times 10^{-7}$ M). In view of the bulk and electrostatic charge of its two 6-substituents, we had not anticipated that OMP-$SO_3$ would be formed spontaneously, or that it would be bound with reasonably high affinity by the enzyme ($K_i = 2.0 \times 10^{-5}$ M). On the basis of the electrostatic stress hypothesis, OMP-$SO_3$ might have been expected to have been excluded from the active site. Instead, OMP-$SO_3$ is bound *more* tightly than UMP-$SO_3$, which has only a single charged substituent.

*Stereochemical Preferences*. Figure 10 compares the affinities of several pyrimidine nucleotide inhibitors of ODCase with the affinities of the substrate and product of decarboxylation, shown at the bottom. The inhibitors are shown in two groups, with unsaturated $C_5{=}C_6$ bonds at the top and with saturated $C_5-C_6$ bonds in the middle.

Each of the three 5,6-saturated inhibitors of ODCase (5,6-dihydro-OMP, 5,6-dihydro-UMP-$SO_3$, and 5,6-dihydro-OMP-$SO_3$) is a mixture of two diastereomers with a chiral center at $C_6$. It remains to be established whether one or both diastereomers of these three compounds are bound at the active site. In each of these molecules, the pyrimidine ring is somewhat puckered because of the presence of a saturated $C_5-C_6$ bond, and the $C_6$ substituents may be axially or equatorially oriented with respect to the dihydropyrimidine ring. Earlier analysis (*20*) of dihydroorotic acid showed that the carboxylate group tends to prefer an axial position, and the crystal structure of 5,6-dihydrouracil-6-sulfonate (*21*) shows the sulfonate group axially oriented at $C_6$. It seems reasonable to suppose that the same may be true of the sulfonyl group of UMP-6-$SO_3$ and of the carboxylate of 5,6-dihydro-OMP. In the case of OMP-$SO_3$, there seems to be no obvious basis for predicting the relative preferences of the $-SO_3^-$ or $-CO_2^-$ groups.[4]

At the glycosidic $C_{1'}-N_1$ bond, pyrimidine nucleotides may adopt either the *syn* (with the $C_2$ carbonyl over the ribose ring) or *anti* (with $C_6$ over the ribose ring) conformation (*22*) (see Table 4). The major structural features of pyrimidine nucleotides that are known to determine their intrinsic *syn*/*anti* preference include steric interactions of the $C_2$ and $C_6$ substituents on the pyrimidine ring, on the one hand, with the $C_{2'}$, $C_{3'}$, and $C_{4'}$ protons and $C_{5'}$ phosphoryl group of ribose, on the other (*23*−*27*). Thus, 5-methyluridine has been shown to adopt the *anti* conformation in which the $C_2$ carbonyl group is rotated away from the substituent ribose, but in contrast, 6-methyluridine adopts the *syn* conformation (with the $C_2$ carbonyl group situated over ribose) because of unfavorable interactions between the 6-methyl group and the ribose $C_{1'}$ proton (*26*). Most of the molecules shown in Figure 10 are equipped with $C_6$ substituents and would therefore be expected to prefer the *syn* conformation. Moreover, $^1$H NMR studies have shown that the substrate OMP (with a carboxylate group at $C_6$) adopts the *syn* conformation in solution, whereas the product UMP (with only a proton at $C_6$) adopts the *anti* conformation (*25*). In all three of the 5,6-dihydro inhibitors, the presence of one or more bulky 6-substituents would be expected to force the nucleotide into the *syn* conformation in solution.

In the crystal structures of ODCase complexes with UMP or OMP (in the latter case, an inactive mutant version of the protein was used), *both* nucleotides are bound in the *syn* conformation (*6*). Thus, ODCase appears to bind OMP with its $C_2$ carbonyl group situated over the ribose ring, while the $C_5{=}C_6$ double bond carrying the scissile carboxylate group faces the catalytic quartet of charged residues. At the active site, decarboxylation presumably generates UMP as the immediate product, in the *syn* conformation that is thermodynamically disfavored in solution. With its release from the active site, UMP reverts to the *anti* conformation that is favored in solution.

The nucleotides in Figure 10 are shown in their known or predicted solution conformations (*syn* or *anti*). Of the inhibitors in Figure 10, all but 6-aza-UMP carry a substituent at $C_6$ and would be expected to be bound in the *syn* conformation. Like UMP, 6-aza-UMP prefers the *anti* conformation in solution (*26*). Interestingly, 6-aza-UMP is bound by ODCase in the *syn* conformation *unless* Ser-127 has been truncated to alanine. Pai and his associates have shown that the S127A mutant protein derived from the ODCase of *Methanobacterium thermoautotropicum* appears to bind 6-aza-UMP in the *anti* conformation (*28*). These authors suggest that the hydroxyl group of Ser-127 forms a strong H-bond to $N_3$ of 6-aza-UMP and that a backbone −NH group forms a H-bond to the 4-carbonyl

[4] In OMP, the carbon atom of the $C_6$ carboxyl group lies in the same plane as the atoms of the pyrimidine ring, but the steric demands of the anomeric $H_{1'}$ atom force the two oxygens to be oriented nearly perpendicular to the ring, so that the $-COO^-$ group is in position to be impacted by electrostatic stress. In contrast, the carboxylate of 5,6-dihydro-OMP or the sulfonate group of 5,6-dihydro-UMP-6-sulfonate can occupy an axial position, potentially relieving the stress (*20*, *21*), but in 5,6-dihydro-OMP-6-sulfonate with the carboxylate group and the sulfonate group on $C_6$, one would expect one of these groups to be equatorial. The crystal structure of 5,6-dihydrouracil-6-sulfonate (*21*) shows that the axial sulfonate group displaces $C_6$ and $N_1$ out of the plane of the other four atoms of the pyrimidine ring by 0.763 and 0.206 Å, respectively. In contrast, the equatorial proton on $C_6$ is oriented downward near the plane of the ring. These observations suggest that the equatorial group of 5,6-dihydro-OMP-6-sulfonate (either the carboxylate or the sulfonate) should be close to the original position of the $C_6$ carboxylate group of OMP.

Table 4: *syn*/*anti* Conformation of UMP Derivatives in Solution and Bound within the Active Site of ODCase

| nucleotide | solution conformation | data[a] | active site bound conformation | data[a] |
|---|---|---|---|---|
| UMP | *anti* | NMR[b−d] comp[m] | *syn* | X-ray[e−g] |
| 6-carboxy-UMP (OMP) | *syn* | NMR[c] comp[l] | *syn* | X-ray[g] |
| 6-carboxamido-UMP | *syn* | predicted | *syn* | predicted |
| 6-cyano-UMP | *syn* | predicted | *syn* | X-ray[k] |
| 6-aza-UMP | *anti* | NMR[b] comp[m,o] | *syn*/*anti* | X-ray[f,g,k,n] |
| 6-thiocarboxamido-UMP | *syn* | predicted | *syn* | predicted |
| 6-oxo-UMP or 6-hydroxy-UMP (BMP) | *anti* syn = anti | NMR[b] comp[m] | *syn* | X-ray[g−j] |
| 5,6-dihydro-6-carboxy-UMP (5,6-dihydro-OMP) | *syn* | predicted | *syn* | predicted |
| 5,6-dihydro-6-sulfonyl-UMP (UMP-$SO_3$) | *syn* | predicted | *syn* | predicted |
| 5,6-dihydro-6-sulfonyl-OMP (OMP-$SO_3$) | *syn* | predicted | *syn* | predicted |

[a] "NMR" or "Comp" indicates that NMR or computational studies, from the references cited, have determined the solution conformation of the nucleotide. "X-ray" indicates that there is an X-ray structure of the nucleotide bound in the active site of ODCase, in the reference provided. "Predicted" indicates the solution conformation is anticipated on the basis of analogy with 6-methyluridine. A large group at $C_6$ would be expected to force the nucleotide into the *syn* configuration to avoid unfavorable interactions between the 6-substituent and the ribose protons and phosphoryl group. [b] Reference *26*. [c] Reference *25*. [d] Reference *23*. [e] Reference *34*. [f] Reference *2*. [g] Reference *35*. [h] Reference *36*. [i] Reference *37*. [j] Reference *38*. [k] Reference *6*. [l] Reference *33*. [m] Reference *32*. [n] 6-Aza-UMP has been shown to be bound by the S127A mutant ODCase in the *anti* conformation. [o] Neutral 6-aza-UMP prefers the *anti* conformation, but its anion exhibits no preference according to computations (*32*).

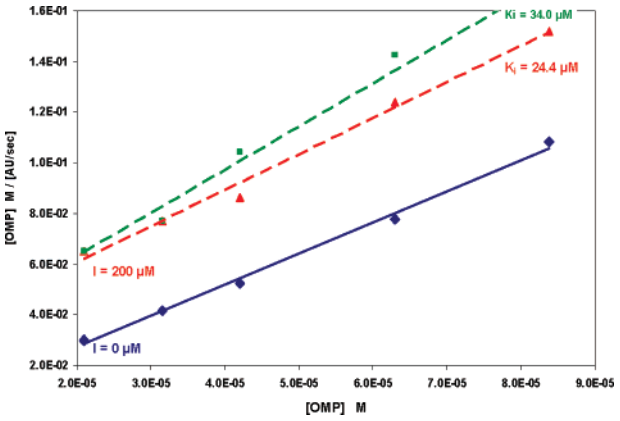


FIGURE 8: Inhibition of ODCase by 200 $\mu$M H-UMP-$SO_3$. ODCase catalyzed decarboxylation of OMP in the absence and presence of 200 $\mu$M H-UMP-$SO_3$. The average $K_i$ was 29.2 $\pm$ 6.8 $\mu$M.

oxygen atom, leading to a preference for the *syn* conformer.

Investigating the effects of sulfur substitution, Shostak and Jones (*29*) showed that 4-thio-OMP exhibits a $K_m$ value of $2 \times 10^{-6}$ M and a $k_{cat}$ value approaching that of OMP. In contrast, 2-thio-OMP exhibits a $K_i$ value of $2.9 \times 10^{-5}$ M and is not decarboxylated by the yeast enzyme. More recent experiments indicate that 2-thio-OMP is bound with a $K_i$ value greater than $10^{-4}$ M (*30*). Smiley and Saleh have attributed the weak binding of 2-thio-OMP to its binding in the "wrong" *anti* conformation (*31*). These investigators have also shown that both 2- and 4- thio-UMP derivatives are competitive inhibitors of ODCase, with $K_i$ values of $2.3 \times 10^{-5}$ and $1.5 \times 10^{-6}$ M, respectively. The differences in binding affinity between 2-thio and 4-thio derivatives of UMP and OMP have been analyzed computationally by Phillips and Lee (*32*) in terms of the relative stabilities of the *syn* and *anti* conformers and the barriers to rotation around the glycosidic bond observed in tetrahydrofuryl derivatives. These authors suggest that 2-thio-UMP, 4-thio-UMP, and 4-thio-OMP exhibit relatively high affinity for the active site because they can be bound in the preferred *syn* conformation. 2-Thio-OMP, which adopts the *anti* conformation in solution and exhibits the highest energy barrier to rotation about the glycosidic bond, cannot rotate easily to the *syn* conformation that may be needed for optimal binding and catalysis. 2-Thio-OMP appears to be the one case in which the bulk of the carboxyl group at $C_6$, relative to that of the C=S group at $C_2$, is insufficient to favor the required *syn* conformation.

The three uridine nucleotides with 6-substituents of varying bulk—the 6-cyano, 6-carboxamido, and 6-thiocarboxamido derivatives of UMP—presumably prefer the *syn* conformation in solution due to the bulk of their $C_6$ substituents. 6-Cyano-UMP has been reported by Fujihashi et al. (*33*) to be "bound in the active site in a manner analogous to that of UMP, 6-azaUMP, and BMP", i.e., the *syn* conformation. Although the structures of their enzyme complexes remain to be established, the 6-carboxamide and 6-thiocarboxamide nucleotides would also be expected to favor the *syn* conformation strongly. An additional pyrimidine nucleotide whose association with ODCase has been examined crystallographically is cytidine 5′-phosphate (CMP) and its 6-carboxylate derivative. CMP adopts the *anti* conformation in solution (*26*) and also within the active site of ODCase where it is very weakly bound (*31*). The 6-carboxylate derivative of CMP was found to be a very poor substrate (roughly $10^5$ less active than OMP) and was only weakly bound (*31*). The weak binding of CMP and CMP-6-carboxylate was ascribed to poor anchoring of the 2′-OH of ribose and to improper positioning of the pyrimidine ring, caused by the presence of the $C_4$ amino group, resulting in greater mobility within the active site.

In the enzyme from a thermophilic bacterium, Pai et al. (*35*) have shown that nucleotides containing xanthine or cytosine are bound in a manner different from that of uracil-based ligands. As noted by the authors, those differences presumably arise from the inordinate size of the purine ring of xanthine and the inability of the cytosine ring to form the conserved H-bonding interactions between the enzyme and the 4-carbonyl group that stabilize the complexes formed

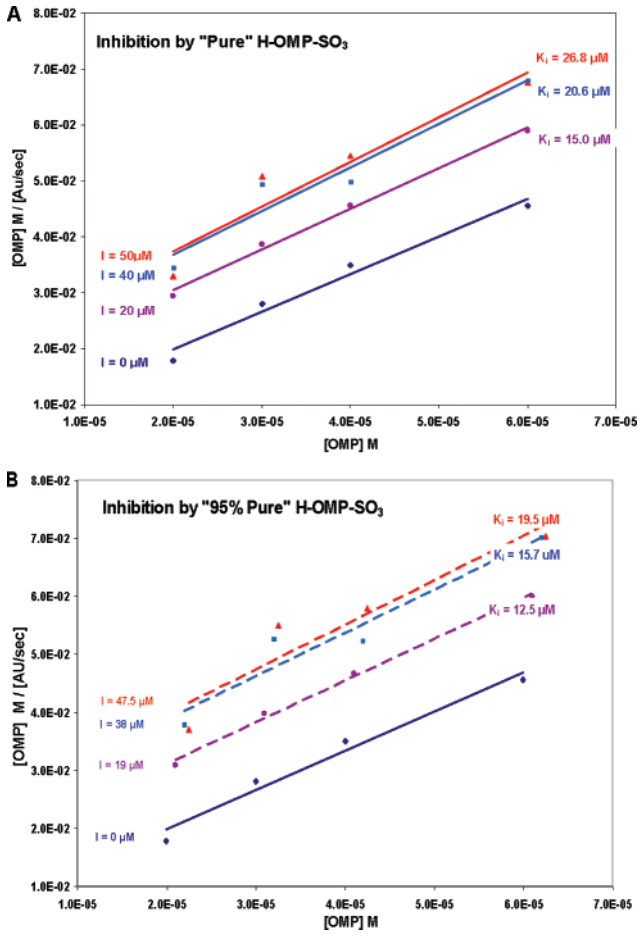


FIGURE 9: Effect of residual OMP in H-OMP-$SO_3$ on $K_i$. $^1$H NMR spectra showed that this preparation of H-OMP-$SO_3$ contained ~5% residual OMP. After the rate data were acquired, the [S]/$v$ vs [S] plots were constructed assuming "pure" (A) and "95% pure" (B) adduct was present in the incubation mixture. In the latter case the concentration of the adduct was reduced by 5% and that 5% was added to the OMP substrate added to the assay mixture. The average of the three $K_i$ values in each situation was 20.8 ± 5.8 $\mu$M assuming pure adduct and 15.9 ± 3.5 $\mu$M for 95% pure adduct. Since the standard deviations of these two $K_i$ values show considerable overlap, this would suggest there is no real effect from the small amount of OMP in the adduct. This is consistent with other tests performed as described in the Results.

by BMP, OMP, and UMP in the published crystal structures of OMP decarboxylase. Instead, the cytosine ring with its 4-amino group is likely to be repelled. Presumably for these reasons, the rings of XMP and CMP are turned away from the binding site normally occupied by the uracil pyrimidine ring, so that the phosphate-binding loop does not close properly, the bases X and C find new H-bonding partners outside the site normally occupied by the substrate and product, and the void remaining at that site is occupied by a molecule of butanediol (in the case of XMP) or five water molecules (in the case of CMP).[5]

The most tightly bound pyrimidine nucleotide inhibitor of ODCase is barbituric acid ribofuranoside 5′-monophosphate (BMP), with an estimated $K_i$ value of $9 \times 10^{-12}$ $M^{-1}$. This triketopyrimidine presents a complex conformational problem, in that the keto groups at $C_2$, $C_4$, and $C_6$ render this molecule nearly symmetrical along the $N_1-C_4$ axis. In principle, each of those keto groups might exist at least to some extent as the hydroxyl tautomer. The accepted structure in solution is equipped with an ionized hydroxyl group (p$K_a$ ≈ 2.8) at $C_6$ and keto groups at $C_2$ and $C_4$. BMP can exist in either the *syn* or *anti* conformation, and $^1$H NMR data indicate that the *anti* conformer predominates in aqueous solution (*26*). In its preference for that *anti* conformation, BMP resembles $\beta$-cyanuric acid ribonucleoside, which is similar in structure to barbituric acid ribonucleoside, but with a third nitrogen atom replacing $C_5$ of the pyrimidine ring (Figure 11).

Phillips and Lee's (*32*) calculations indicate that the *syn* and *anti* conformers of BMP are similarly favorable energetically and are separated by a high barrier to rotation about the glycosidic bond. When bound at the active site of ODCase, BMP has been found to be in the *syn* conformation, which orients the $C_6$ oxyanion facing the catalytic tetrad of alternating aspartate and lysine residues (*1*). It is possible that ODCase selects the *syn* conformer of BMP from solution or that the enzyme induces the *anti* conformer of BMP to rotate about the glycosidic bond to be bound in the *syn* conformation. If BMP were bound to any extent as the rare triketo species, then $C_5$ would carry two geminal protons (as in the three 5,6-dihydro inhibitors) and the true $K_d$ value of that rare species would be even lower than the measured $K_i$ value. The geminal $C_5$ protons of the triketo form would be difficult to observe by $^1$H NMR spectra because they would presumably be subject to solvent exchange through keto−enol equilibration (*39*, *40*).

On the basis of these considerations and modeling of several complexes of ODCase from *M. thermoautotrophicum* containing various uracil derivatives (Supporting Information), we present hypothetical structures of UMP-$SO_3$ and OMP-$SO_3$ bound within the active site of the enzyme (Figure 12). These structures are derived from the well-characterized complex of ODCase with BMP and structural data for 5,6-dihydrouracil-6-sulfonate (*21*). The puckered dihydropyrimidine ring of each adduct is oriented in such a way as to be superimposed on the pyrimidine ring of BMP as closely as possible. The phosphoribosyl groups are not altered. The sulfonate group is axial to the puckered dihydropyrimidine ring. Negatively charged sulfonate and carboxylate groups are located close to Lys-72 (within ~3 Å) and are likely to experience a strong Coulombic interaction. When the protein

[5] The binding of XMP and that of CMP by ODCase, in which the whole nucleotide is rotated out of the active site, represent interesting exceptions. A reviewer has suggested that the present sulfonate derivatives may also be bound in unfamiliar ways. In the absence of direct structural information, we agree that the possibility of radically different modes of binding cannot be dismissed. We note, however, that the uracil derivatives shown in black and blue in Figure 10 have H-bonding capabilities that are similar to each other, but very different from those of CMP. The published atomic coordinates of BMP, OMP, UMP, 6-iodo-UMP, and 6-aza-UMP bound at the active site of ODCase show that the uracil rings overlie each other and that the phosphoribose groups are all similarly aligned. Further, the hydrogen bond interactions between the enzyme and each ligand are found to be the same. For those reasons, we consider it probable that the present inhibitors, shown in red in Figure 10, are bound in approximately the same way as BMP, OMP, and UMP. That mode of binding would allow these negatively charged inhibitors to interact favorably with the positively charged lysine at the active site, and our inspection of the published crystal structures of BMP, OMP, or UMP complexes with ODCase suggests that there should be no steric impediment to binding of the present inhibitors in the same manner as BMP and UMP. (See the Supporting Information for the details of the interactions between ODCase and various nucleotides.)

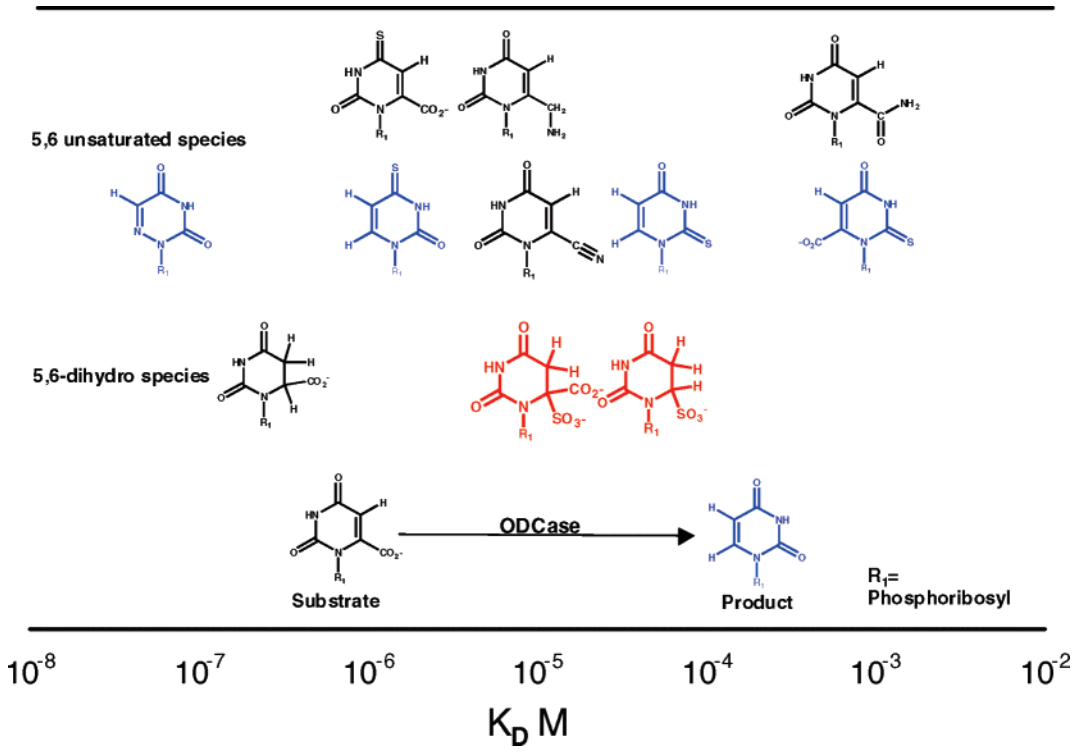


FIGURE 10: Dissociation constants for UMP derivatives bound by ODCase shown in the known or predicted *solution conformation*, *syn* (black structures) or *anti* (blue structures) about the glycosidic bond (the vertical bar below $N_1$ in each structure to $C_{1'}$ of the phosphoribosyl moiety, abbreviated as $R_1$). The nucleotides are in three groups: substrate and product (bottom row), 5,6-saturated or 5,6-dihydro nucleotides (middle row), and 5,6-unsaturated nucleotides (two topmost rows). Two of the tightest binding nucleotides, BMP ($K_D = 9 \times 10^{-12}$ $M^{-1}$) (*45*) and 6-thiocarboxamido-UMP ($K_D = 3.5 \times 10^{-9}$ $M^{-1}$) (*46*), are not shown. Dissociation constants ($M^{-1}$) for the nucleotides in the figure are (4-thio-OMP) $2 \times 10^{-6}$ (*29*), (6-methylamino-UMP) $3.3 \times 10^{-6}$ (*7*), (6-carboxamido-UMP) $6 \times 10^{-4}$ (*46*), (6-aza-UMP) $6 \times 10^{-8}$ (*4*), (4-thio-UMP) $1.5 \times 10^{-6}$ (*31*), (6-cyano-UMP) $2.9 \times 10^{-5}$ (*42*), (2-thio-UMP) $2.3 \times 10^{-5}$ (*31*), (2-thio-OMP) $>10^{-4}$ (*30*), (5,6-hydro-OMP) $2.5 \times 10^{-7}$ (*47*), (5,6-dihydro-OMP-6-$SO_3$) $2 \times 10^{-5}$ (this work), (5,6-dihydro-UMP-6-$SO_3$) $2.9 \times 10^{-5}$ (this work), (OMP) $7 \times 10^{-7}$ (*4*), and (UMP) $2 \times 10^{-4}$ (*4*).

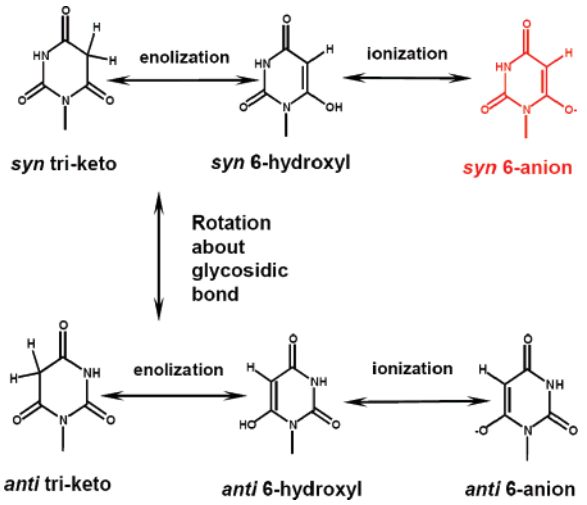


FIGURE 11: Some of the conformers and ionic species of BMP. Although BMP is equally likely to be *syn* or *anti* in aqueous solution (*31*), the triketo species, shown on the left side of the figure, is only observed in nonaqueous solutions. The *syn* 6-anion of BMP (highlighted in red) is the only species bound within the active site of ODCase.

surface was included in parts B and C of Figure 12, the sulfonate group projected slightly into the protein surface in the vicinity of Lys-72. The other protein side chain close to the sulfonate group is Met 126, but this side chain is flexible. In view of the flexibility in the lysine and methionine side chains, there appears to be little steric impediment with the axial sulfonyl group. These tentative structural conjectures remain to be tested by exact structural methods.

*Conflicting Structural Requirements of a Commodious—yet Discriminating—Active Site*. In the absence of direct structural information, comparison of the behavior of the nucleotides discussed above suggests several inferences of the binding properties of the 6-sulfonate inhibitors described here. On the basis of their observed tight binding, it seems reasonable to suppose that the sulfonate adducts of UMP and OMP are bound in the *syn* conformation, like OMP, UMP, and other nucleotides that are tightly bound. Apparently, the carboxylate binding pocket, which may be the initial location for the $CO_2$ molecule released from OMP, is large enough to accommodate a sulfonate group as well as a carboxylate group. The puckered 5,6-dihydropyrimidine ring may not position $C_6$ and its substituents as deeply in the carboxylate pocket as does the planar pyrimidine ring of OMP, with its coplanar carboxylate group, but 5,6-dihydro-OMP is bound with an affinity comparable with that of the substrate OMP, suggesting that the pocket can accommodate a noncoplanar 6-substituent. Saturation of the $C_5{=}C_6$ bond of OMP converts the substrate into an inhibitor that does not undergo enzymatic decarboxylation. The sulfonate adduct of OMP is bound ~30 times less tightly than OMP itself, but the sulfonate adducts of UMP are bound ~7-fold more tightly than the product UMP. It seems evident that both negative charge at $C_6$ and $C_5{-}C_6$ saturation of the pyrimidine are readily accommodated by the active site of ODCase.

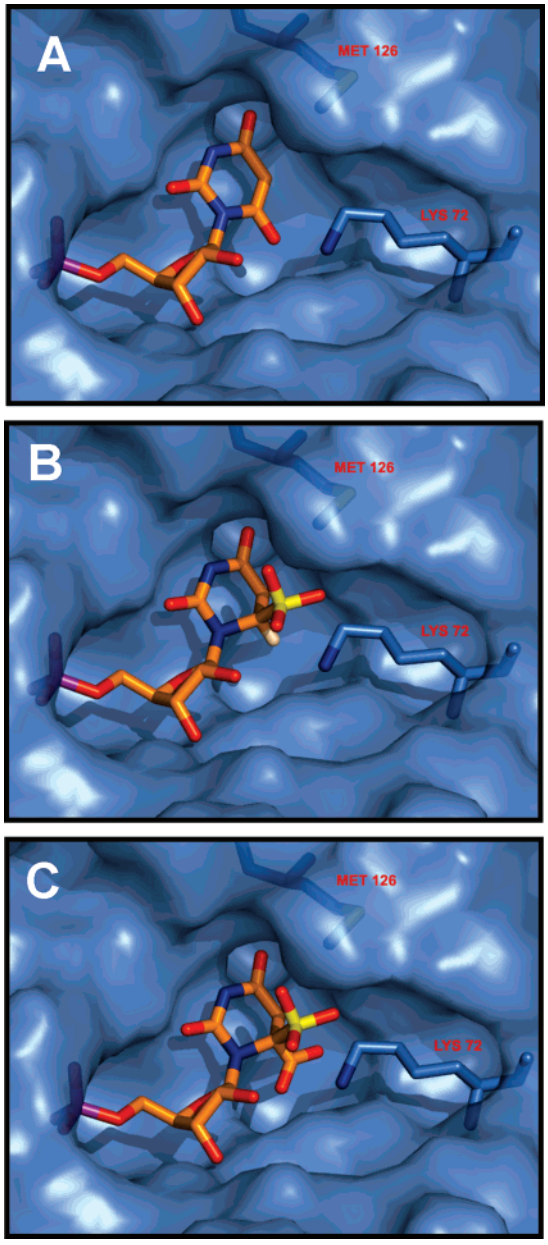


FIGURE 12: Hypothetical binding of the UMP-$SO_3$ and OMP-$SO_3$ inhibitors in the active site of ODCase based on the binding of BMP. (A) BMP bound in ODCase from *M. theromoautotrophophicum* from ref *35*. The protein surface around Lys-72 has been removed to expose the amino acid side chain. Met-126 is inside the surface above carbons 4 and 5 of the pyrimidine ring. (B) UMP-$SO_3$ modeled into the active site using BMP as the basic structure, with modification of the pyrimidine ring and the position of the sulfonate group based on the X-ray structure of sodium 5,6-dihydrouracil-6-sulfonate from ref *21*. The sulfonate group is axially oriented coming up from the pyrimidine ring toward the viewer. Two of the three sulfonate oxygens are within 3 Å of the nitrogen of the $NH_2$ group of Lys-72. The $C_6$ proton is shown in tan color. (C) OMP-$SO_3$ modeled into the active site using the structure in (B) with the carboxyl group replacing the proton on $C_6$ in the equatorial position and retaining the sulfonate group in the axial position. In both (B) and (C) the negatively charged sulfonate and carboxylate groups are in close proximity to the positively charged Lys-72. An alternative structure with the pyrimidine ring puckered in the opposite direction for both adducts caused unfavorable interactions between the sulfonate group and a proline residue in the bottom of the cavity. Figures and modeled inhibitors were generated using PyMol (DeLano Scientific LLC; Palo Alto, CA) and PDB entry 1LOR for the BMP complex in panel A, which was modified, as described above, to produce panels B and C.

The present observations, and an earlier report of the inhibition of ODCase by 6-methylamino-UMP (*8*), raise serious questions about the "electrostatic stress" mechanism as originally proposed (*2*). According to that mechanism, the carboxylate group of Asp-70 repels the 6-carboxylate group of OMP in such a way as to destabilize it, advancing the reaction toward a transition state from which $CO_2$ departs as the $C_6$ anion of UMP is generated. If electrostatic destabilization of the enzyme−substrate complex constituted an important part of such a mechanism, one might have expected that sulfonate adducts (especially OMP-$SO_3$) would tend to be excluded from the active site because of the greater size and charge density of the carboxylate and sulfonate substituents at $C_6$. Instead, these sulfonate adducts are bound almost as tightly as OMP and 5,6-dihydro-OMP. The behavior of the three 5,6-dihydro compounds indicates that ODCase can accommodate nonplanar pyrimidine rings. Moreover, several of the pyrimidine nucleotides in Figure 10 are equipped with 6-substituents that vary in structure, number of atoms, and electrostatic charge, but are bound with similar affinities. Those are not the properties that one would expect of an active site with a rigid structure that imposes sufficient electrostatic stress on the substrate to produce a major advancement along the reaction coordinate.

In contrast to the overall similarity of the binding affinities summarized in Figure 10, the affinity of ODCase for the altered substrate in the transition state (which probably resembles a $C_6$ carbanion, in which an electron pair replaces the substrate's $C_6$−$COO^-$ group) is vastly higher than its affinity for OMP in the ground state. The remarkable magnitude of that increase in affinity ($\sim 10^{17}$-fold) requires that the enzyme−substrate interactions be extremely strong and intimate in the transition state. That unusual jump in affinity is partly reflected in the affinity of BMP ($K_i = 10^{-11}$ M), in which a $C_6$−$CO^-$ group replaces the substrate's $C_6$− $COO^-$ group. What is most striking about this series ($C_6^-$ > $C_6$−$O^-$ > $C_6$−$COO^-$) is that binding affinity increases very steeply with decreasing size, whereas electrostatic charge remains nominally unchanged. When the negative charge is separated from $C_6$ by zero, one, or two bonds, the free energy of binding changes from −31.7 to −15.0 to −8.4 kcal/mol.

Perhaps these paradoxical properties of the active site (indiscriminate binding of substrates and their analogues in the ground state, but highly discriminating binding of the altered substrate in the transition state) can be reconciled if we suppose that in the transition state (to a much greater extent than in the ground state) the active site closes around the substrate in such a way as to provide the intimate and discriminating contacts that are required for catalysis (*43*). It seems reasonable to conjecture that these changes are reflected to some extent in the crystallographically observed ordering and closing of loop 207−217 of the yeast enzyme that accompanies the binding of BMP. After entry of the substrate, at a rate that approaches the diffusion limit (*4*), the closure of that loop permits new H-bonding interactions between the substrate phosphoryl group and the active site, notably Tyr-217. For such a loop movement to support catalysis, it is necessary that the cost of distorting the enzyme from its native "open" structure be less than the benefit of enhanced attractive forces between the enzyme and substrate in the transition state. That overriding benefit would seem

to be possible if (a) loop closure involves the relative movement of parts of the active site that are intrinsically somewhat ordered (*43*) and (b) there is a high level of synergism between the forces of attraction that are work in the transition state, but not the ground state.

In apparent agreement with that sequence of events, the phosphoryl group of OMP has been shown by its presence to contribute a factor of $10^{11}$ to the value of $k_{cat}/K_m$ observed for OMP (*5*, *44*). Moreover, the phosphite ion has been shown to enhance, by a factor of $10^8$, the reactivity of a truncated form of the nucleoside orotidine (*48*). Just as ODCase produces one of the larger rate enhancements that is known to be produced by any enzyme, the substrate phosphoryl group (although spatially distant from the site of substrate decarboxylation) produces the largest effect of a simple substituent that appears to have been reported for any enzyme reaction. These effects, and the present findings, seem to be compatible with the view that much of the rate enhancement produced by this unusual catalyst arises mainly from its ability to stabilize the altered substrate in the transition state, rather than from electrostatic destabilization of the ground-state enzyme−substrate complex.

## ACKNOWLEDGMENT

We thank Dr. Gottfried Schroeder for helpful discussions and assistance in the preparation of the PyMol figures.

## SUPPORTING INFORMATION AVAILABLE

Analysis of the binding interactions between ODCase and five uracil-based nucleotides as well as XMP and CMP to compare and contrast the interactions, supporting the proposal that UMP-$SO_3$ and OMP-$SO_3$ are most likely bound like other uracil nucleotides, as illustrated in Figure 12. This material is available free of charge via the Internet at http://pubs.acs.org.

## REFERENCES

1. Houk, K. N., Tantillo, D. J., Stanton, C., and Hu, Y. (2003) What Have Theory and Crystallography Revealed About the Mechanism of Catalysis by Orotidine Monophosphate Decarboxylase? in *Topics in Current Chemistry 238: Orotidine Monophosphate Decarboxylase: A Mechanistic Dialogue* (Lee, J. K., and Tantillo, D. J., Eds.) pp 1−22, Springer-Verlag, New York.
2. Wu, N, Mo, Y., Gao, J., and Pai, E. F. (2000) Electrostatic Stress in Catalysis: Structure and Mechanism of the Enzyme Orotidine Monophosphate Decarboxylase, *Proc. Natl. Acad. Sci. U.S.A. 97*, 2017−*2022*.
3. Traut, T. W., and Temple, B. R. S. (2000) The Chemistry of the Reaction Determines the Invariant Amino Acids during the Evolution and Divergence of Orotidine 5′-Monophosphate Decarboxylase, *J. Biol. Chem. 275*, 28675−28681.
4. Miller, B. G., Snider, M. J., Short, S. A., and Wolfenden, R. (2000) Contribution of Enzyme−Phosphoribosyl Contacts to Catalysis by Orotidine 5′-Phosphate Decarboxylase, *Biochemistry 39*, 8113−8118.
5. Sievers, A., and Wolfenden, R. V. (2005) The Effective Molarity of the Substrate Phosphoryl Group in the Transition State for Yeast OMP Decarboxylase, *Bioorg. Chem. 33*, 45−52.
6. Miller, B. G., Snider, M. J., Wolfenden, R., and Short, S. A. (2001) Dissecting a Charged Network at the Active Site of Orotidine 5′-Phosphate Decarboxylase, *J. Biol. Chem. 18*, 15174−15176.
7. Wu, N., Gillon, W., and Pai, E. F. (2002) Mapping the Active Site-Ligand Interactions of Orotidine 5′-Monophosphate Decarboxylase by Crystallography, *Biochemistry 41*, 4002−4011.
8. Callahan, B. P., and Wolfenden, R. (2004) OMP Decarboxylase: An Experimental Test of Electrostatic Destabilization of the Enzyme−Substrate Complex, *J. Am. Chem. Soc. 126*, 14698−14699.
9. Shapiro, R., Servis, R. E., and Welcher, M. (1970) Reactions of Uracil and Cytosine Derivatives with Sodium Bisulfite: A Specific Deamination Method, *J. Am. Chem. Soc. 92*, 422−424.
10. Hayatsu, H., Wataya, Y., Kai, K., and Iida, S. (1970) Reaction of Sodium Bisulfite with Uracil, Cytosine, and Their Derivatives, *Biochemistry 9*, 2858−2865.
11. Hayatsu, H., Wataya, Y., and Kai, K. (1970) The Addition of Sodium Bisulfite to Uracil and Cytosine, *J. Am. Chem. Soc. 92*, 724−726.
12. Erickson, R. W., and Sander, E. G. (1972) General Acid-Base Catalysis of the Reversible Addition of Bisulfite to 1,3-Dimethyluracil, *J. Am. Chem. Soc. 94*, 2086−2091.
13. Sander, E. G., and Deyrup, C. L. (1972) The Effect of Bisulfite on the Dehalogenation of 5-Chloro-, 5-Bromo-, 5-Iodouracil, *Arch. Biochem. Biophys. 150*, 600−605.
14. Sedor, F. A., Jacobson, D. G., and Sander, E. G. (1974) The Addition of Bisulfite to 5-Fluorouracil. Evidence for a Change in Rate Determining Step, *Bioorg. Chem. 3*, 221−228.
15. Rork, G. S., and Pitman, I. H. (1974) Elimination of Bisulfite Ion from a Series of Uracil- Bisulfite Adducts: Evidence for a Two-Step Mechanism, *J. Am. Chem. Soc. 96*, 4654−4663.
16. Pitman, I. H., and Jain, N. B. (1979) Covalent Addition of Bisulfite Ion to N-Alkylated Uracils and Thiouracils, *Aust. J. Chem. 32*, 545−552.
17. Triplett, J. W., Smith, S. L., Layton, W. J., and Digenis, G. A. (1977) Carbon-13 Nuclear Magnetic Resonance Investigations into the Interactions of Bisulfite with Pyrimidine Nucleosides and Nucleotides, *J. Med. Chem. 20*, 1594−1597.
18. Porter, D. J. T., and Short, S. A. (2000) Yeast Orotidine -5′-Phosphate Decarboxylase: Steady State and Pre-Steady State Analysis of the Kinetic Mechanism of Substrate Decarboxylation, *Biochemistry 39*, 11788−11800.
19. Triplett, J. W., Digenis, G. A., Layton, W. J., and Smith, S. L. (1978) Carbon-13 Nuclear Magnetic Resonance Studies of Bisulfite-Pyrimidine Addition Reactions: Stereoselective Formation and Reactions of the 5-Halouridines, *J. Org. Chem. 43*, 4411−414.
20. Katritzky, A. R., Nesbit, M. R., Kurtev, B. J., Lyapova, M., and Pojarlieff, I. G. (1969) $\beta$-Ureido Acids and Dihydrouracils−VII Applications of Proton Resonance Spectroscopy−XXXII; NMR Spectra and Conformation of Dihydrouracils and Related Compounds, *Tetrahedron 25*, 3807−3824.
21. Barnes, C. L., and Hawkinson, S. W. (1980) Sodium 5,6-Dihydrouracil-6-sulfonate Monohydrate, *Acta Crystallogr., B 36*, 2431−2433.
22. Donohue, J. and Trueblood, K. N. (1960) Base Pairing in DNA, *J. Mol. Biol. 2*, 363−371.
23. Blackburn, B. J., Grey, A. A., Smith, I. C. P., and Hruska, F. (1970) Determination of the Molecular Conformation of Uridine in Aqueous Solution by Proton Magnetic Resonance Spectroscopy. Comparison with $\beta$-Pseudouridine, *Can. J. Chem. 48*, 2866−2870.
24. Dugas, H., Blackburn, B. J., Robins, R. K., Deslauriers, R., and Smith, I. C. P. (1971) A Nuclear Magnetic Resonance Study of $\beta$-Cyanuric Acid Riboside. Further Evidence for the Anti Rotamer in Pyrimidine Nucleosides, *J. Am. Chem. Soc. 93*,468−3470.
25. Hruska, F. E. (1971) Molecular Conformation of Orotidine, a Naturally Occurring Nucleoside, in the Syn Conformation in Aqueous Solution, *J. Am. Chem. Soc. 93*, 1795−1797.
26. Schweizer, M. P., Banta, E. B., Witkowski, J. T., and Robins, R. K. (1973) Determination of Pyrimidine Nucleoside Syn, Anti Conformational Preference in Solution by Proton and Carbon-13 Nuclear Magnetic Resonance, *J. Am. Chem. Soc. 95*, 3770−3778.
27. Follmann, H., Pfeil, R., and Witzel, H. (1977) Pyrimidine Nucleosides in Solution: A Study of Intramolecular Forces by Proton Magnetic Resonance Spectroscopy, *Eur. J. Biochem. 77*, 451−461.
28. Wu, N., and Pai, E. F. (2004) Crystallographic Studies of Native and Mutant Orotidine 5′-Phosphate Decarboxylases, in *Topics in Current Chemistry 238: Orotidine Monophosphate Decarboxylase: A Mechanistic Dialogue* (Lee, J. K., and Tantillo, D. J., Eds.), pp 23−42, Springer-Verlag, New York.
29. Shostak, K., and Jones, M. E. (1992) Orotidylate Decarboxylase: Insights into the Catalytic Mechanism from Substrate Specificity Studies, *Biochemistry 31*, 12155−12161.

30. Smiley, J. A., Hay, K. M., and Levison, B. S. (2001) A Reexamination of the Substrate Utilization of 2-Thioorotidine 5′-Monophosphate by Yeast Orotidine-5′-Monophosphate Decarboxylase, *Bioorg. Chem. 29*, 96−106.
31. Smiley, J. A., and Saleh, L. (1999) Active Site Probes for Yeast OMP Decarboxylase: Inhibition Constants of UMP and Thio-Substituted UMP Analogues and Greatly Reduced Activity Toward CMP-6-Carboxylate, *Bioorg. Chem. 27*, 297−306.
32. Phillips, L. M., and Lee, J. K. (2005) Theoretical Studies of the Effect of Thio Substitution on Orotidine Monophosphate Decarboxylase Substrates, *J. Org. Chem. 70*, 1211−1221.
33. Fujihashi, M., Bello, A. M., Poduch, E., Wei, L., Annedi, S. C., Pai, E. F., and Kotra, L. P. (2005) An Unprecedented Twist to ODCase Catalytic Activity, *J. Am. Chem. Soc. 127*, 15048−15050.
34. Appleby, T. C., Kinsland, C., Begley, T. P., and Ealick, S. E. (2000) The Crystal Structure and Mechanism of Orotidine 5′-Monophosphate Decarboxylase, *Proc. Natl. Acad. Sci. U.S.A. 97*, 2005−2010.
35. Wu, N., and Pai, E. F. (2002) Crystal Structures of Inhibitor Complexes Reveal an Alternate Binding Mode in Orotidine-5′-Monophosphate Decarboxylase, *J. Biol. Chem. 277*, 28080−28087.
36. Miller, B. G., Hassell, A. M., Wolfenden, R., Milburn, M. V., and Short, S. A. (2000) Anatomy of a Proficient Enzyme: The Structure of Orotidine 5′-Monophosphate Decarboxylase in the Presence and Absence of a Potential Transition State Analog, *Proc. Natl. Acad. Sci. U.S.A. 97*, 2011−2016.
37. Harris, P., Poulsen, J.-C. N., Jensen, K. F., and Larsen, S. (2000) Structural Basis for the Catalytic Mechanism of a Proficient Enzyme: Orotidine 5′-Monophosphate Decarboxylase, *Biochemistry 39*, 4217−4224.
38. Poulsen, J.-C. N., Harris, P., Jensen, K. F., and Larsen, S. (2000) Selenomethionine Substitution of Orotidine-5′-Monophosphate Decarboxylase Causes a Change in Crystal Contacts and Space Group, *Acta Crystallogr., D 57*, 1251−1259.
39. Jones, A. J., Grant, D. M., Winkley, M. W., and Robins, R. K. (1970), Carbon-13 Magnetic Resonance. XVIII. Selected Nucleotides, *J. Phys. Chem. 74*, 2684−2689.
40. Otter, B. A., Falco, E. A., and Fox, J. J. (1969) Nucleosides. LVIII. Transformations of Pyrimidine Nucleosides in Alkaline Media. III. The Conversion of 5-Halogenouridines into Imidazoline and Barbituric Acid Nucleosides. *J. Org. Chem. 34*, 1390−1396.
41. Lee, T-S, Chong, L. T., Chodera, J. D., and Kollman, P. A. (2001) An Alternative Explanation for the Catalytic Proficiency of Orotidine 5′- Phosphate Decarboxylase, *J. Am. Chem. Soc. 123*, 12837−12848.
42. Poduch, E., Bello, A. M., Tang, S., Fujihashi, M., Pai, E. F., and Kotra, L. P. (2006) Design of Inhibitors of Orotidine Monophosphate Decarboxylase Using Bioisosteric Replacement and Determination of Inhibition Kinetics, *J. Med. Chem. 49*, 4937−4945.
43. Wolfenden, R. (1974) Enzyme Catalysis: Conflicting Requirements of Substrate Access and Transition State Affinity, *Mol. Cell. Biochem. 3*, 207−211.
44. Miller, B. G., Butterfoss, G. L., Short. S. A., and Wolfenden, R. (2001) Role of Enzyme−Ribofuranosyl Contacts in the Ground State and Transition State for Orotidine 5′-Phosphate Decarboxylase: A Role for Substrate Destabilization?, *Biochemistry 40*, 6227−6232.
45. Levine, H. L., Brody, R. S., and Westheimer, F. H. (1980) Inhibition of Orotidine-5′-phosphate Decarboxylase by 1-(5′-Phospho-$\beta$-D-ribofuranosyl)barbituric Acid, 6-Azauridine 5′-Phosphate and Uridine 5′-Phosphate, *Biochemistry 19*, 4993−4999.
46. Landesman, P. W. (1982) Design, Synthesis and Evaluation of Potential Inhibitors of Pyrimidine Biosynthesis: A Mechanistic Approach, Ph.D. Thesis, University at Buffalo, Buffalo, NY.
47. Miller, B. G., and Wolfenden, R. (2002) Catalytic Proficiency: The Unusual Case of OMP Decarboxylase, *Annu. Rev. Biochem. 71*, 847−885.
48. Amyes, T. L., Richard, J. P., and Tait, J. J. (2005) Activation of Orotidine 5′-Monophosphate Decarboxylase by Phosphite Dianion: The Whole is the Sum of Two Parts, *J. Am. Chem. Soc. 127*, 15708−15709.

BI700796T